中国光学（中英文）
Chinese Optics
核心期刊

Generation of a high spectral power supercontinuum covering the ultraviolet to infrared by a femtosecond laser multi-filament array in fused silica

GUO Ya-jun, WANG Jian-ji

Citation:
GUO Ya-jun, WANG Jian-ji. Generation of a high spectral power supercontinuum covering the ultraviolet to infrared by a femtosecond laser multi–filament array in fused silica[J]. *Chinese Optics*, 2026, 19(5): 1–10. doi: 10.3724/CO.EN–2026–0005
郭亚军, 王健吉. 飞秒激光多丝阵列在熔融石英中生成覆盖紫外至红外波段的高光谱功率超连续[J]. 中国光学, 2026, 19(5): 1–10. doi: 10.3724/CO.EN–2026–0005

View online: https://doi.org/10.3724/CO.EN–2026–0005

第 19 卷　第 5 期
2026 年 9 月

中国光学（中英文）
Chinese Optics

Vol. 19　No. 5
Sept. 2026

文章编号　2097-1842(2026)05-0001-10

Generation of a high spectral power supercontinuum covering the ultraviolet to infrared by a femtosecond laser multi-filament array in fused silica

GUO Ya-jun, WANG Jian-ji*

(*Jilin University of Chemical Technology*, *School of Science*, *Jilin*, 132022, *P.R. China*)

* *Corresponding author*, *E-mail*: *wangjianji@jluct.edu.cn*

Abstract: Supercontinuum (SC) generated from femtosecond laser filamentation has found extensive applications due to its broadband spectral properties. In this study, we present a novel method to simultaneously improve the spectral coverage and power density of SC. This is realized by combining two-color femtosecond laser injection and multi-filament array arrangement in fused silica. With this method, high spectral power SC is obtained. The spectral power density is above 0.1 mW/nm over a broad wavelength range from approximately 380 nm to 950 nm. We find that both the spectral range and power density of SC are affected by the input power and the intensity ratio between the fundamental and second-harmonic laser pulses. In addition, the spectral fluctuation of the generated SC is measured to be less than 4% within 6 minutes. These results offer a feasible and effective way to enhance the spectral power and coverage of SC sources. They are of great importance for promoting the practical applications of SC.

Key words: supercontinuum; filamentation; self-phase modulation; spectral cumulative effect

飞秒激光多丝阵列在熔融石英中生成覆盖紫外至红外波段的高光谱功率超连续

郭亚军, 王健吉*

(吉林化工大学 理学院, 吉林 吉林 132022)

摘要:为了实现飞秒激光成丝超连续辐射的光谱参数优化, 使用了透镜阵列聚焦双色飞秒激光在熔融石英块中成丝的方法产生超连续辐射。对超连续辐射光谱功率密度的提高、光谱范围的拓宽、光谱分布特性的调节等方面进行研究。首先, 比较了不同波长的飞秒激光输入对成丝超连续辐射光谱范围的影响。接着, 以透镜阵列替代单透镜聚焦飞秒激光成丝, 通过多丝阵列形成的光谱累积效应提升超连续辐射的光谱功率密度。然后, 实验比较了输入激光功率对超连续辐射

收稿日期:2026-01-12; **修订日期:**xxxx-xx-xx

基金项目:吉林省自然科学基金资助项目(No. YDZJ202401639ZYTS); 吉林省教育厅资助项目(No. JJKH20240300KJ, No. JJKH20240299KJ)

Supported by the Natural Science Foundation of Jilin Province (No.YDZJ202401639ZYTS); the Education Department of Jilin Province (No. JJKH20240300KJ, No. JJKH20240299KJ).

光谱分布的影响,实现了对超连续辐射高频区域(或低频区域)光谱功率密度的独立控制。最后,对该方法产生的超连续辐射光谱稳定性进行了评价。实验结果表明:该方法可以获得在高频光谱范围增强的超连续辐射,并且在 380 nm~950 nm 的光谱范围内功率密度均高于 0.1 mW/nm。该方式产生的超连续辐射可以灵活优化光谱功率密度、光谱范围和光谱分布的特性,以适应超连续辐射光谱的实际应用需求。

关　键　词:超连续;飞秒激光成丝;自相位调制;光谱累积效应

中图分类号:Q437.5;O433　**文献标志码:**A　**doi:**10.3724/CO.EN-2026-0005　**CSTR:**32171.14.CO.EN-2026-0005

1 Introduction

Femtosecond laser filamentation has been widely utilized in laser wavelength conversion via nonlinear optical processes, including third-harmonic generation[1] and terahertz (THz) wave emission[2]. The SC generated by femtosecond laser filamentation in a transparent Kerr media arises from self-phase modulation (SPM), ionization, and self-steepening effects[3]. Intense SC or white-light sources have become efficient tools in many fields and have attracted considerable attention owing to their promising applications, including remote sensing[4-5], biomedical imaging[6], ultra-wideband supercontinua generation[7] and pulse self-compression[8]. These applications demand SC sources with broad spectral coverage, extended cutoff wavelength, and high intensity. Numerous efforts have been devoted to optimizing the properties of SC (white light source)[9-12]. Generally, a higher spectral power density can expand the application scope of SC and endow it with broader prospects. The nonlinear coefficient of the condensed media such as fused silica is higher than that of air[13], leading to a higher electron density during the filamentation. Meanwhile, the self-steepening effect also plays an important role in SC generation[3]. Therefore, SC generation in the solid medium such as fused silica, is more efficient[14]. However, the low damage threshold of fused silica[15] restricts the generation of SC with high spectral power. A novel technique for generating intense SC using multi-thin plates has been demonstrated[16-17]. Another efficient method is to form a multi-filament distribution via a micro-lens array (MLA) to enhance the SC spectrum. This approach can not only overcome the drawback of the low damage threshold of the solid medium but also enable the accumulation of spectral broadening effect, leading to a significant enhancement of SC intensity[18]. Unlike the multi-thin-plate technique, which requires a long propagation distance of several meters, intense SC generated by femtosecond laser induced multi-filament arrays in solids with a MLA can shorten the working distance to a few centimeters. In addition, many other convenient methods have been proposed to generate multi-filament arrays[19-22]. Therefore, femtosecond laser multi-filamentation in fused silica is a promising candidate for enhancing the spectral power of SC.

On the other hand, broadening the spectral coverage of SC and enhancing the power in specific wavelength ranges are critical for its practical applications. For instance, synthesizing sub-cycle scale light fields requires a high-intensity, nearly uniform SC with a broad spectral range[23]. The nonlinear response of gas media driven by two-color fields has been reported as a competitive candidate for generating broadband SC by bridging the continuum spectra of each color component[24]. This method has also been employed to generate SC covering the ultraviolet-to-millimeter waveband[7] or ultra-broadband white-light pulses with an energy of approximately 0.6 mJ[16]. It can be expected that multi-filament distribution in fused silica driven by multi-color femtosecond lasers could serve as an effective way to generate ultra-broadband SC with high spectral power.

In this work, we propose a scheme to generate broadband SC with high spectral power covering the UV to near-IR region. This is achieved by using a two-color femtosecond laser drive a multi-filament distribution in fused silica via a MLA. We compare the multi-filament patterns in fused silica and the far-field laser spots for input pulses of different wavelengths. Our results show that the two-color laser method significantly broadens the spectral coverage of the SC. Furthermore, we investigate the effect of the MLA-induced multi-filament distribution on the accumulation of SC power. A high-spectral-power supercontinuum extending from the UV to the IR is obtained, and the relationship between the input power and the SC spectral power is analyzed. We also study the influence of the power ratio between the two input pulses on the spectral structure by varying the input power of the fundamental frequency and second-harmonic pulse. As a result, the spectral power density in the UV and IR wings can be readily modulated.

2 Experimental setup

The schematic illustration of our experimental setup is shown in Fig. 1. The front-end source is a Ti: sapphire chirped-pulse amplification (CPA) system (Spectra-Physics: Spitfire Ace), which operates with a pulse duration of 50 fs at a central wavelength of 800 nm. This system delivers pulse energy exceeding 2.5 mJ energy at a repetition rate of 1 kHz. The laser beam is split into two beams by a beam splitter. The frequence of one femtosecond laser beam is doubled to 400 nm using a BBO crystal. The two femtosecond laser beams at 800 nm and 400 nm are combined by a dichroic mirror. The maximum powers of the fundamental laser (800 nm) and second-harmonic laser (400 nm) are 750 mW and 430 mW, respectively. The combined beam is then focused by a commercial 10×10 MLA with a pitch of 1.015 mm and a focusing distance of 218.3 mm to generate a multi-filament array in the fused silica. The dimensions of the bulk fused silica are 50 mm×30 mm×30 mm. For comparison, the SC generated by a single lens with a focal length of f=200 mm is also investigated. A charge-coupled device (CCD) camera (PI: PIXIS 1024) is used to record the filamentation images, with an integration time of CCD is 50 ms. The SC emission is collected by a lens with a focal length of f=75 mm into a spectral detection system for SC characterization. A spectrograph (Ocean Optics: USB4000) is employed to record the SC spectra. A neutral density filter is used to attenuate the SC signal and aviod saturation during the measurement. Each spectrum is obtained by accumulating 50 laser pulses.

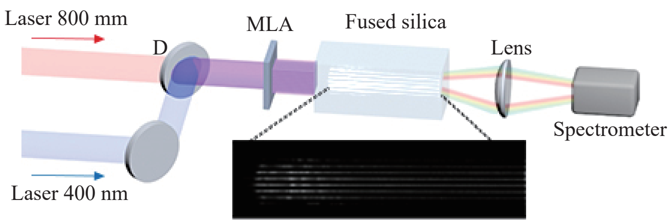

Fig. 1 Experimental setup. Two femtosecond laser pulses at 800 nm and 400 nm are combined by a dichroic mirror. The combined beam is focused into fused silica using a commercial 10×10 MLA. D: dichroic mirror with high reflectivity at 400 nm and high transmission at 800 nm

图 1 实验装置。两个波长分别为 800 nm 和 400 nm 的飞秒激光脉冲通过二向色镜进行合束。组合光束使用商用 10×10 MLA 聚焦到熔融石英中。D: 在 400 nm 波长处具有高反射率, 在 800 nm 波长处具有高透射率的二向色镜

3 Results and discussion

Femtosecond laser filamentation can be formed in fused silica when a single lens is used as the focusing element. Figure 2(a) shows the typical SC emission intensities from filamentation in fused silica for femtosecond laser pulse at different wavelengths: 400 nm (P=20 mW), 800 nm (P=

50 mW), and 400 nm+800 nm (P=70 mW). The spectra of the fundamental-frequency (800 nm) and frequency-doubled (400 nm) input laser pulses are plotted in Fig. 2(a). The difference in spectral width between fundamental-frequency pulse (800 nm) and frequency-doubled pulse (400 nm) in Fig. 2(a) is obvious. When a laser pulse with a central wavelength of 800 nm propagates through a BBO crystal, the spectral width of the generated 400 nm second-harmonic pulse is significantly compressed. This occurs because, under the effect of chromatic dispersion, only the components near the central wavelength satisfy the phase-matching condition for second-harmonic generation, whereas the other components are effectively suppressed. Therefore, the spectral width of fundamental-frequency pulse (800 nm) is broader than that of the frequency-doubled pulse (400 nm). A similar spectral width distribution can be observed in Ref.[16]. In addition, Zeng et al. experimentally demonstrated that the spectral width of frequency-doubled laser can be further compressed using phase modulation technologies[25-26]. The fused silica block is placed 180 mm away from the single lens. The laser pulse energy is limited to less than tens of microjoules to avoid damaging the fused silica. For either 400 nm or 800 nm pulse alone, the spectral width of the SC generated by a single lens is broader than that of the input pulses, as shown in Fig. 2(a). The spectral range is mainly concentrated on both sides of the input pulse's center wavelength. The farther from the center wavelength, the lower the spectral intensity. The SC spectral of fundamental-frequency pulse (800 nm) and the second-harmonic pulse (400 nm) hardly overlap in the spectral region with significant intensity. It can be seen that simultaneous filamentation using both the fundamental and second-harmonic pulse (400 nm+800 nm) can effectively extend the SC spectral range. The SC spectral range (cyan line) generated by two-color laser filamentation in fused silica is much wider than that generated by the 400 nm pulse (blue line) and 800 nm pulse (yellow line) alone. In addition, the spectral intensity near 500 nm under two-color laser excitation is higher than that under single color pulse input. This enhancement near 500 nm can be attributed to the superposition of spectral components from both pulses. Both the SC generated by the fundamental-frequency pulse and that generated by the second-harmonic pulse have low intensity near 500 nm, but their spectra are non-negligible; when a two-color laser pulse is used to generate SC, these two spectral components around 500 nm superimpose on each other, leading to an obvious intensity enhancement at this wavelength. In contrast, the SC generated by the fundamental-frequency pulse (800 nm) has negligible intensity around 400 nm, so the SC generated by the two-color laser pulse near 400 nm is not significantly higher than that generated by the 400 nm pulse alone.

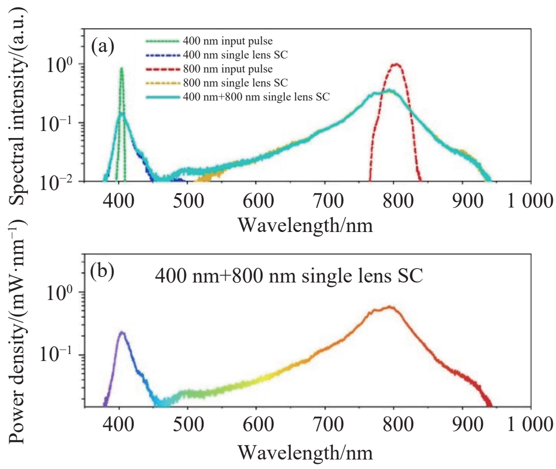

Fig. 2 (a) Spectral intensity profiles of the 400 nm and 800 nm input pulses, as well as the SC generated by the 400 nm, 800 nm and 400+800 nm laser pulses, respectively. (b) Spectral power density distribution of SC generated via two-color pulse 400 nm+800 nm focused by a single lens

图 2 (a) 400 nm 和 800 nm 输入脉冲的光谱强度分布，以及分别由 400 nm、800 nm 和 400+800 nm 激光脉冲产生的超连续谱。(b) 通过单透镜聚焦的双色脉冲 400 nm+800 nm 产生的超连续谱的光谱功率密度分布

The corresponding spectral power density of the broadband SC driven by the two-color pulse is calculated and plotted in Fig. 2(b). Although two-color laser driving can broaden the SC spectral range of filamentation in fused silica, the spectral power density in most of the spectral range is much lower than 0.1 mW/nm, except for the regions close to the central wavelengths of the input pulses. This indicates that when a single lens is used for SC generation, the limited spectral power of the SC still restricts its practical applications.

To enhance the spectral power of the SC emission, we use an MLA as the focusing element to generate a multi-filament array in fused silica. It has been demonstrated that using an MLA enables manipulation of the filamentation pattern with incident 800 nm laser pulse of very high energy without damaging the sample. Consequently, SC generation with a higher power and similar spectral broadening can be achieved compared to that obtained with a single focusing lens[18]. It can be expected that regardless of the input pulse's wavelength, the cumulative effect of SC generated by the multi-filament array will always exist to enhance the spectral power. The multi-filament patterns of different wavelengths formed by MLA imaging on the screen are shown in Fig. 3(a), and the corresponding photos of the far-field laser spots are displayed in Fig. 3(b). We note that the incident laser at 400 nm produces slightly more filaments at the periphery of the beam than the 800 nm laser does. in Fig. 3(a). This is because the plasma produced during femtosecond laser filamentation primarily arises from multi-photon ionization. The photon energy of 400 nm laser pulse is twice that of 800 nm laser pulse. For a given ionization energy of the medium, the 400 nm laser exhibits a higher probability of multiphoton ionization. Although the energy transmitted through the microlens array at the beam periphery decreases in both cases, the 400 nm laser, with its higher photon energy, is expected to possess a lower threshold power for filamentation. Therefore, the 400 nm laser generates a greater number of filaments than the 800 nm laser in our experiment. The results in Fig. 3(a) and (b) demonstrate that the colors of the multi-filament patterns and the laser pulse spot images are governed by the wavelength of the incident laser pulse. The color features associated with filamentation in fused silica further reflect the spectral composition of the SC, as documented in Ref.[27]. The objective of recording multi-filament array imaging and SC patterns for various incident lasers is to compare how the input laser wavelength affects the colors of the filaments and SC beams. Under the influence of diffraction, the cross-sectional profile size of the SC beam gradually spreads as

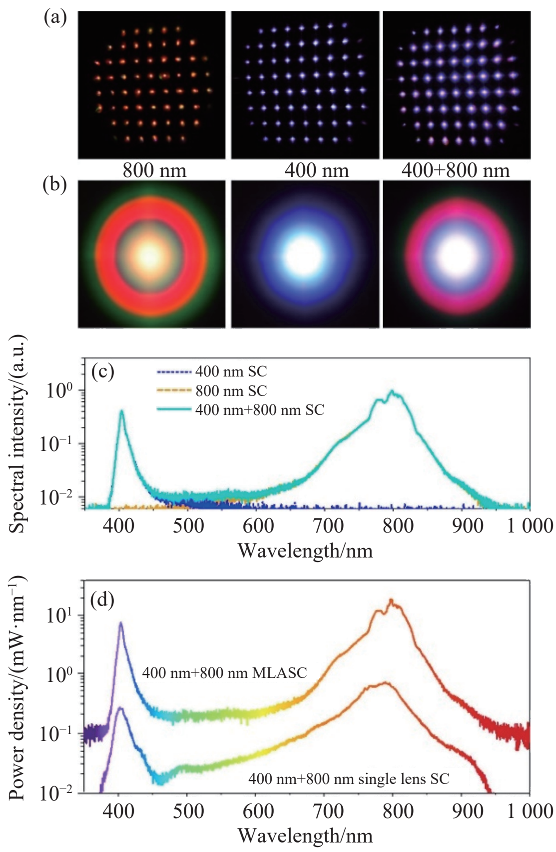

Fig. 3　(a) Image of the multi-filament array cross-section and (b) the corresponding SC beams. (c) SC spectral intensity profiles induced by a MLA element for femtosecond laser pulses of different wavelengths: 800 nm, 400 nm, and 400 nm+800 nm, respectively. (d)Spectral power density distributions of SC generated via two-color pulse focused by a single lens and MLA, respectively

图 3　(a) 多丝阵列横截面图像和 (b) 对应的超连续光束。(c) 由微透镜阵列元件聚焦不同波长飞秒激光脉冲(分别为 800 nm、400 nm 和 400 nm+800 nm)产生的超连续光谱强度分布。(d) 由单透镜和微透镜阵列分别聚焦双色脉冲产生的超连续光谱功率密度分布

the propagation distance increases. The spatial sizes of the multi-filament array images and SC beam profiles don't affect the spectral data. So we just set the white screen at an arbitrary distance far away behind the fused silica block for conveniently.

Figure 3(c) presents the intensity distributions of the SC associated with multi-filament induced by focusing the fundamental laser pulse (800 nm), the second-harmonic pulse (400 nm), and their combined pulse (400 nm + 800 nm) through an MLA, respectively. Compared with the cases where one of the two beams is blocked, the spectra range of the SC is broader when both beams are present simultaneously. Generally, the spectral intensity is low in the near-UV range of the SC generated by the near-IR (800 nm) femtosecond laser pulse filamentation is relatively low. As shown in Fig. 3(c), when the fundamental pulse and the second-harmonic pulse (400 nm+800 nm) are used simultaneously to generate SC via MLA, the spectral intensity in the UV range is significantly enhanced (cyan line) compared with that generated by the 800 nm fundamental laser pulse alone (yellow line). In our experiment, the cross-sectional images of multi-filament array shown in Fig.3 (a), the SC beams depicted in Fig. 3(b), and the SC spectra illustrated in Fig. 3(c) were not acquired simultaneously. Initially we placed an imaging lens along the laser path behind the fused silica block to project the cross-sectional distribution of the multi-filament array onto a white screen. Subsequently, we employed a color digital camera to capture the images of multi-filament array (a) generated by different input lasers. For the SC beams (b), we directly projected them onto a white screen and also recorded them using a digital camera. The acquisition of SC spectra was conducted utilizing the scheme outlined in Fig. 1.

The multi-filament array formed by the two-color femtosecond laser pulse enables the generation of SC with high spectral power. We also calculated the spectral power density of the SC generated by combining two-color beams with the MLA, as shown in Fig. 3(d). As demonstrated in Fig. 3(d), when compared with using a single lens case, the spectral power density has been significantly enhanced across the entire range of the SC. The cumulative effect of SC produced by the multi-filament array plays a pivotal role. It should be noted that the cumulative effect of SC produced by the multi-filament array results from spatially coherent superposition[18], which differs from the SC accumulation along the longitudinal direction of a femtosecond filament focused by a single lens[28]. As we known, the SC generated by the filaments is coherent white light, and the SC sub-sources produced by individual filaments will experience constructive interference with one another, thereby augmenting the spectral power of the SC. The larger the number of independent filaments, the more SC sub-sources participate in spectral accumulation. Thus, increasing the number of filaments at a fixed laser incident power can enhance the conversion efficiency and spectral power of the SC.

Figure 4(a) compares the SC spectral curves driven by the two-color femtosecond laser at different total powers P. The power ratio between the second-harmonic and fundamental beams is approximately fixed at 0.57, consistent with the power ratio used in Fig. 3(d). Our results indicate that both the spectral power density and spectral coverage of the SC are dependent on the input power. Figure 4(b) presents the corresponding SC spectral distribution as as a function of the total power P. As illustrated in Figs. 4(a) and (b), increasing the input power broadens both wing sides of the SC spectral range and enhances the spectral power density across the entire SC coverage. Using this approach, we obtained an ultra-broadband SC with high spectral power under our experimental conditions, covering a spectral range of approximately 380 nm to 950 nm. The spectral power density exceeds 0.1 mW/nm across the entire coverage range, with a two-orders-of-magnitude enhancement at certain wavelengths within SC spectrum.

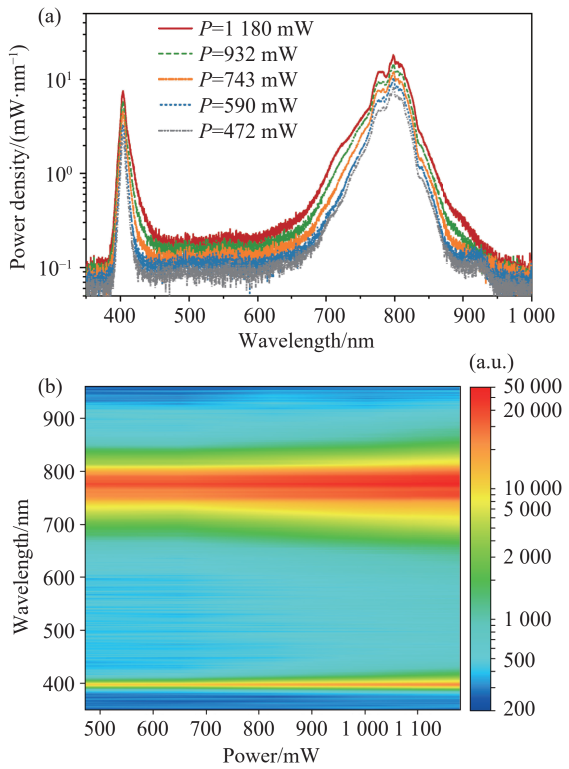

Fig. 4　(a) Typical SC spectral power density profiles of the two-color femtosecond laser pulse passing through the MLA with different total powers P: 1 180 mW, 932 mW, 743 mW, 590 mW, and 472 mW, respectively. (b) SC spectral distribution as a function of laser pulse power

图 4　(a) 双色飞秒激光脉冲在不同总功率 P 下通过微透镜阵列产生的典型超连续谱功率密度分布：功率分别为 1 180 mW、932 mW、743 mW、590 mW 和 472 mW。(b) 超连续谱分布随激光脉冲功率的变化

We also manipulated the spectral intensity distribution of the SC by varying the power of the IR and UV components of the input two-color laser pulse, as shown in Fig. 5. Figure 5(a) presents the spectral distribution obtained by individually adjusting the input power P_r of the fundamental-frequency laser while fixing the input power P_b of the second-harmonic laser, and vice versa in Fig. 5(b). As expected, the red wing of the SC is sensitive to the input power of the fundamental-frequency laser (Fig. 5(a)), while exerting a minor effect on the blue wing. In contrast, the input power of the second-harmonic laser has a significant impact on the blue wing of the SC (Fig. 5(b)). Thus, the spectral power density of the SC can be selectively adjusted on either the red or blue side by controlling the input power of a specific component. Our results demonstrate that a femtosecond laser pulse with a much broader frequency range propagating through an MLA element can generate high-power SC with a wider spectral range, and the spectral distribution of the SC can also be modulated by controlling the input power ratio of each component.

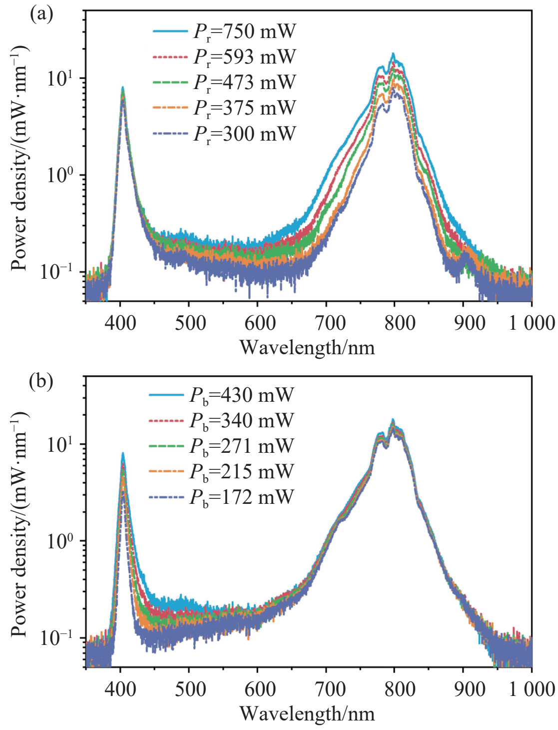

Fig. 5　High-spectral-power-density SC profiles obtained by varying the power of a specific component of the input two-color laser pulse: (a) varying the fundamental frequency laser power P_r (750 mW, 593 mW, 473 mW, 375 mW, 300 mW) while fixing the second-harmonic laser power P_b; (b) varying the second-harmonic laser power P_b (430 mW, 340 mW, 271 mW, 215 mW, 172 mW) while fixing the fundamental frequency laser power P_r

图 5　通过改变输入双色激光脉冲特定组分的功率获得的高光谱功率密度超连续分布：(a)改变基频激光功率 P_r(750 mW、593 mW、473 mW、375 mW、300 mW)，同时固定二次谐波激光功率 P_b；(b)改变二次谐波激光功率 P_b(430 mW、340 mW、271 mW、215 mW、172 mW)，同时固定基频激光功率 P_r。

Finally, we evaluated the spectral stability of the high-spectral-power SC source generated in our experiment. As shown in Fig. 6, the temporal evolutions of the counts in several pixels corresponding to the specific wavelengths (380 nm, 500 nm, 530 nm, 550 nm, 600 nm, and 650 nm) were used to assess the spectral power stability of the SC.

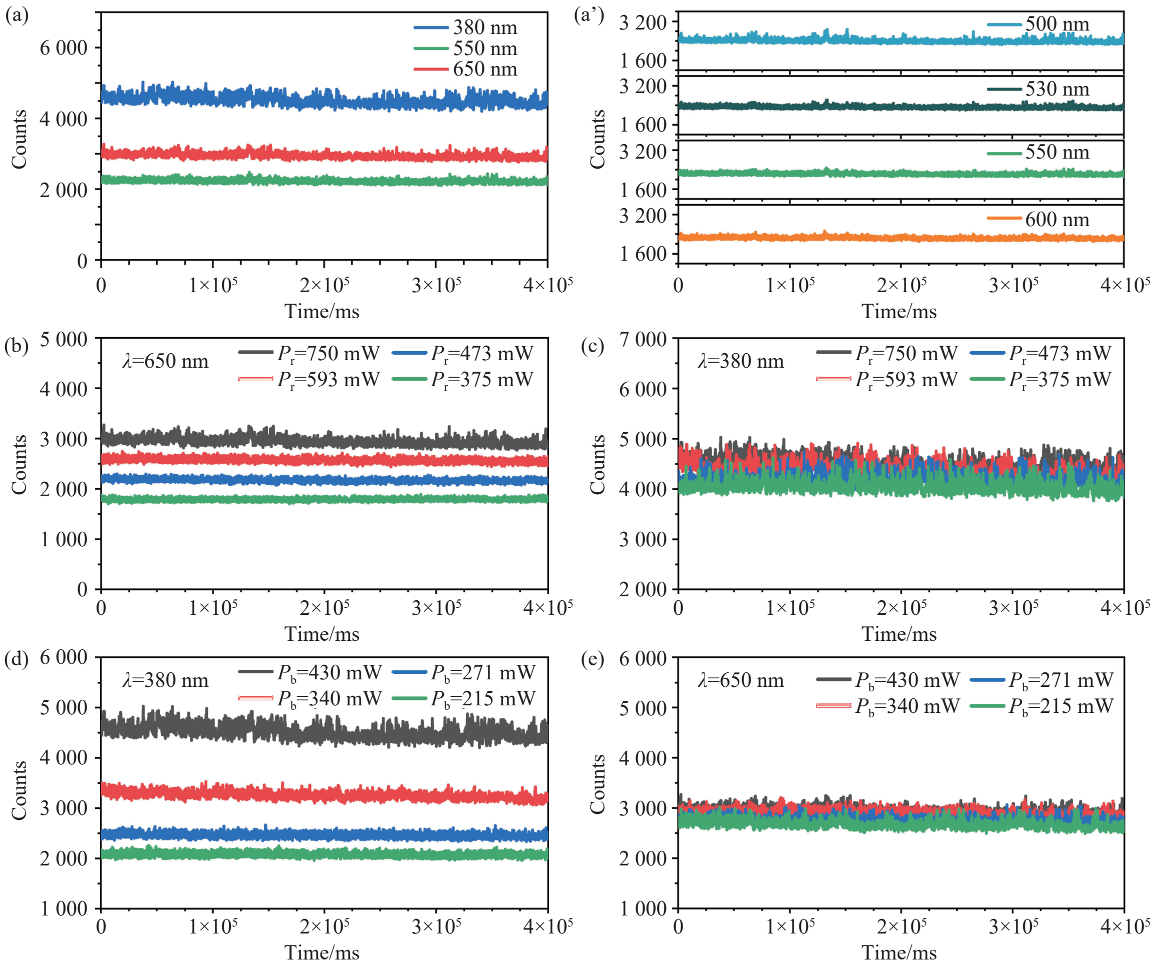

Fig. 6 Spectral stability of the high power SC source generated by the two-color pulse in our experiment. (a) and (a') show the SC spectral stability of the different typical wavelengths: 380 nm, 500 nm, 530 nm, 550 nm, 600 nm, 650 nm. (b) and (c) depict the temporal evolution of the spectral counts at 650 nm and 380 nm, respectively, over the same time period by varying the fundamental laser power P_r=750 mW, 593 mW, 473 mW, and 375 mW. (d) and (e) show the spectral counts at 650 nm and 380 nm, respectively, over the same time period by varying the second-harmonic laser power P_b=430 mW, 340 mW, 271 mW, and 215 mW

图 6 我们使用双色脉冲在实验中产生的高功率超连续谱的光谱稳定性。(a)和(a')展示了超连续中不同典型波长(380 nm、500 nm、530 nm、550 nm、600 nm、650 nm)的光谱稳定性。(b)和(c)分别描绘了通过改变基频激光功率 P_r =750 mW、593 mW、473 mW 和 375 mW，在同一时间段内 650 nm 和 380 nm 处的光谱计数的时间演化。(d)和(e)分别展示了通过改变二次谐波激光功率 P_b =430 mW、340 mW、271 mW 和 215 mW，在同一时间段内 650 nm 和 380 nm 处的光谱计数

Figures 6(a) and (a') present the temporal evolutions of the signal intensity for different wavelengths at a total input power of P=1 180 mW (P_r=750 mW and P_b=430 mW). Under this condition, all signal intensities remained stable, showing nearly straight lines with only a slight drop over 6 minutes—indicating that the SC spectrum exhibits consistent stability across various wavelength ranges. As illustrated in Fig. 6(a'), for several wavelengths in the range of 500 nm to 600 nm, the count value stabilized around 2000. This is consistent with the spectral distribution shown in Fig. 4(a), where, in the flat spectral range of 480 nm to 620 nm, each component exhibits nearly the same spectral power density.The influence of the input power of each component on spectral stability was also investigated. As shown in Figs. 6(b)–(c), we measured the temporal evolutions of spectral intensity over the same time period by varying the fundamental pulse power P_r; similarly, Figs. 6(d)-(e) show the temporal evolutions when varying the second-harmonic pulse power P_b. Our results indicate that the input powers of the fundamental and second-harmonic lasers have a minor effect on the stability of the SC, with a noticeable trend that lower input laser powers correspond to better SC spectral stability. As expected, the intensity of the SC is significantly influenced by the input laser power, as demonstrated in Figs. 6(b)–(e). Furthermore, adjusting the input power of the fundamental laser exerts a greater influence on the SC intensity in the red wing than in the blue wing, as shown in Figs. 6(b)–(c). In contrast, when adjusting the input power of the second-harmonic laser pulse, the input power has opposite effects on the red and blue wings of the SC. Additionally, the spectral fluctuation of the SC was evaluated to be less than 4% over a 6-minute period.

4 Conclusion

In summary, we have demonstrated a new method for generating a high spectral power SC covering the UV to IR region. This method uses a MLA to produce a multi-filament array in fused silica driven by a two-color femtosecond laser. Compared with the SC generated by a near-infrared pulse with a center wavelength of 800 nm, the addition of a 400 nm pulse not only broadens the SC coverage but also significantly increases the SC spectral intensity on the UV side. Additionally, the cumulative effect of the multi-filament array enhances the spectral power density across the entire spectral coverage. An ultra-broadband high power density SC was obtained. Under our experimental conditions, the spectral power density exceeds 0.1 mW/nm across the entire SC coverage, with a spectral intensity nearly two orders of magnitude higher near the incident laser wavelengths. Furthermore, the input power of each injection component directly affects the spectral power density of the corresponding SC spectral range. By separately varying the input power of the fundamental and second-harmonic beams, modulate the spectral power density in the red or blue wing of the SC spectrum. In addition, the stability of the SC produced by our scheme was also evaluated. Due to the multi-filament accumulation effect enhancing the SC power-density and the two-color input pulse broadening the spectral range, the synergy of these effects can be further amplified by using a larger-scale multi-filament array with multi-color femtosecond laser injection, enabling the generation of a higher-power ultra-broadband SC.

References:

[1] YIN F K, LIU Y X, WANG T J, *et al.*. Improving the beam pointing and intensity stability of the third harmonic generated in air filament[J]. *Optics & Laser Technology*, 2025, 181: 111717.

[2] GUO H CH, DU H L, ZHAN Q, *et al.*. Dominance of plasma-induced modulation in terahertz generation from gas filament[J]. *Optics Express*, 2024, 32(3): 4277-4294.

[3] GAETA A L. Catastrophic collapse of ultrashort pulses[J]. *Physical Review Letters*, 2000, 84(16): 3582-3585.

[4] RAY P, MEDIĆ T, SALIDO-MONZÚ D, *et al.*. High-precision hyperspectral laser scanning for improved radiometric correction of backscatter intensity[J]. *Optical Engineering*, 2024, 63(5): 054110.

[5] RAY P, SALIDO-MONZÚ D, CAMENZIND S L, *et al.*. Supercontinuum-based hyperspectral LiDAR for precision laser scanning[J]. *Optics Express*, 2023, 31(20): 33486-33499.

[6] DE LA CADENA A, PARK J, TEHRANI K F, *et al.*. Simultaneous label-free autofluorescence multi-harmonic microscopy driven by the supercontinuum generated from a bulk nonlinear crystal[J]. *Biomedical Optics Express*, 2024, 15(2): 491-505.

[7] MITROFANOV A V, SIDOROV-BIRYUKOV D A, NAZAROV M M, *et al.*. Ultraviolet-to-millimeter-band

supercontinua driven by ultrashort mid-infrared laser pulses[J]. *Optica*, 2020, 7(1): 15-19.
[8] SAVITSKY I V, VORONIN A A, STEPANOV E A, *et al*.. Sub-cycle pulse revealed with carrier-envelope phase control of soliton self-compression in anti-resonant hollow-core fiber[J]. *Optics Letters*, 2023, 48(17): 4468-4471.
[9] SALCEDO-RODRIGUEZ C A, GALLEGOS-ARELLANO E, ESTUDILLO-AYALA J M, *et al*.. Numerical analysis of spectroscopic studies using supercontinuum generated by noise-like pulses[J]. *Results in Physics*, 2025, 74: 108298.
[10] HWANG J, PARK S, KO K, *et al*.. Quantitative gas pressure measurement by molecular spectroscopy using chip-based supercontinuum in the mid-infrared[J]. *Optics Express*, 2023, 31(22): 35624-35631.
[11] MUNIZ-CÁNOVAS P, BARMENKOV Y, RESÉNDIZ-CÓRDOVA Á A, *et al*.. The use of a supercontinuum light source for the characterization of passive fiber optic components[J]. *Open Physics*, 2024, 22(1): 20240092.
[12] WANG J L, DING B, WU Q F, *et al*.. Spectral optimization of the three-primary laser-based displays with large circadian action factor based on age of user[J]. *IEEE Photonics Journal*, 2024, 16(6): 6700109.
[13] TZORTZAKIS S, SUDRIE L, FRANCO M, *et al*.. Self-guided propagation of ultrashort IR laser pulses in fused silica[J]. *Physical Review Letters*, 2001, 87(21): 213902.
[14] COUAIRON A, MYSYROWICZ A. Femtosecond filamentation in transparent media[J]. *Physics Reports*, 2007, 441(2-4): 47-189.
[15] NGUYEN N T, SALIMINIA A, LIU W, *et al*.. Optical breakdown versus filamentation in fused silica by use of femtosecond infrared laser pulses[J]. *Optics Letters*, 2003, 28(17): 1591-1593.
[16] SU Y B, FANG SH B, GAO Y T, *et al*.. Efficient generation of UV-enhanced intense supercontinuum in solids: toward sub-cycle transient[J]. *Applied Physics Letters*, 2021, 118(26): 261102.
[17] GAO Y T, SU Y B, XU S Y, *et al*.. Generation of annular femtosecond few-cycle pulses by self-compression and spatial filtering in solid thin plates[J]. *Optics Express*, 2021, 29(19): 29789-29801.
[18] CAMINO A, HAO Z Q, LIU X, *et al*.. High spectral power femtosecond supercontinuum source by use of microlens array[J]. *Optics Letters*, 2014, 39(4): 747-750.
[19] GUO Y J, WANG J J, SONG X W, *et al*.. Gaseous pre-lattice assisted supercontinuum enhancement of femtosecond laser filamentation[J]. *Physics of Plasmas*, 2021, 28(7): 072303.
[20] WANG J J, GUO Y J, SONG X W, *et al*.. Multi-dimensional control of femtosecond laser filaments by inserting a wedge plate in the forced focusing region[J]. *Physics of Plasmas*, 2022, 29(1): 012301.
[21] GUO Y J, WANG J J, SONG X W, *et al*.. The generation and control of serpentine femtosecond laser filament array[J]. *Optics Communications*, 2022, 522: 128605.
[22] WANG J J, GUO Y J, SONG X W, *et al*.. Manipulation of femtosecond laser multi-filament array by spatiotemporal phase modulation[J]. *Optics Communications*, 2021, 495: 127113.
[23] CORKUM P B, ROLLAND C, SRINIVASAN-RAO C. Supercontinuum generation in gases[J]. *Physical Review Letters*, 1986, 57(18): 2268-2271.
[24] BÉJOT P, KASPARIAN J, WOLF J P. Dual-color co-filamentation in Argon[J]. *Optics Express*, 2008, 16(18): 14115-14127.
[25] ZENG X, CUI SH ZH, CHENG X, *et al*.. Spectral compression by phase doubling in second harmonic generation[J]. *Optics Letters*, 2022, 47(2): 222-225.
[26] RUAN B W, ZENG X, FENG Y. Modeling of a second harmonic spectrum in passive phase demodulation[J]. *Applied Optics*, 2023, 62(11): 2809-2814.
[27] HAO Z Q, STELMASZCZYK K, ROHWETTER P, *et al*.. Femtosecond laser filament-fringes in fused silica[J]. *Optics Express*, 2011, 19(8): 7799-7806.
[28] ZHANG L ZH, XI T T, HAO Z Q, *et al*.. Supercontinuum accumulation along a single femtosecond filament in fused silica[J]. *Journal of Physics D: Applied Physics*, 2016, 49(11): 115201.

Author Biography:

GUO Ya-jun (1991—), female, born in Changchun, Jilin Province, she received her Ph.D. from Changchun University of Science and Technology in 2022. Her research primarily focuses on the theoretical and experimental studies of femtosecond laser filamentation, as well as investigations into strong nonlinear effects on laser propagations through refractive-modulated medium. E-mail: guoyajun@jluct.edu.cn